Journal of Materials Chemistry C

Accepted Manuscript

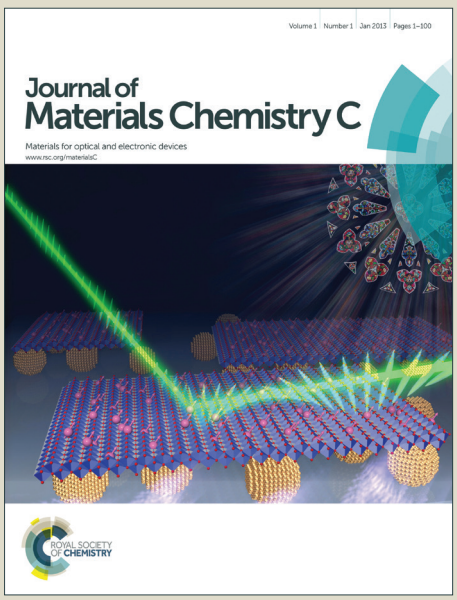

ROYAL SOCIETY OF CHEMISTRY

www.rsc.org/materialsC

Journal Name

RSCPublishing

ARTICLE

Main-chain Chirality and Photophysical Property Relations in Chiral Conjugated Polymers

Chao Zheng,[a] Zhongfu An, [a] Yosuke Nakai,[b] Taiju Tsuboi,*[, b, c] Yang Wang, [a] Huifang Shi, [a,c] Runfeng Chen,*[, a] Huanhuan Li, [a] Yimu Ji, [a] Junfeng Li, [a] Wei Huang*[, a, c]

Cite this: DOI: 10.1039/xoxxoooooox

Received 6th February 2014,
Accepted

DOI: 10.1039/xoxxoooooox

www.rsc.org/

A series of *R*- and *S*- binaphthyl-containing polyfluorenes, bearing different content and type of axial chirality in main-chain, have been synthesized through Suzuki polycondensation to investigate the influence of the covalently incorporated chirality on the photophysical properties of chiral conjugated polymers. The experimental measurements by UV-Vis and photoluminescence (PL) spectra, cyclic voltammetry, and circular dichroism spectroscopy, reveal that the chiral copolymers possess high thermostablity, high luminescence efficiency, reversible electrochemical property, and intrachain transferred dichroism; surprisingly, the *R*-chiral polymers exhibit better spectral thermostability, stronger suppressing ability upon theβ-phase formation of the main-chain, and higher PL quantum efficiency than *S*-chiral polymers in solid film. The theoretical insights by either *ab initio* density functional theory (DFT) calculations or molecular dynamic (MD) simulations suggest that these differences are probably resulted from the more planar chain conformation of *S*-chiral polymers, which leads to stronger interchain interaction and increased tendency to form low efficient and unstable excimers or quenches. The different effects of enantiomers on the photophysical properties of chiral conjugated polymers may provide an import update on the understandings of chiroptics.

Introduction

Chirality plays a fundamental part in the activities of biological molecules and broad classes of chemical reactions and interactions[1], providing a wide range of potential applications in pharmacy[2], chrial separation[3], enantioselective sensor[4], asymmetrical catalysis and reaction[5], and nonlinear optics[6]. The addition of a chiral compound into an achiral polymer is one of the most promising means to introduce chirality to a polymer[7]. Successful attempts to plant chirality covalently into the backbone of the widely used and optically and electronically active π-conjugated polymers have produced exciting features for the both sides, resulting in a new generation optoelectronic material of chiral conjugated polymers.[8-10]

Take the widely available chiral 1,1'-binaphthyls as an example. Since the 1990s, when Pu's laboratory started systematic investigations on these axial chiral compounds[11], various main-chain chiral conjugated polymers have been prepared by covalently incorporating the biaryl-conjugated and highly stable chiral 1,1'-binaphthyl into the main-chain of a variety of conjugated polymers[7, 12-14] including arylenvinylenes, arylenes, aryleneethylnylenes, thiophenes, fluorenes, etc. The chirality of 1,1'-binaphthyl is generally well preserved, transferred, or even amplified in the corresponding chiral conjugated polymers[15], which are attractive for advanced applications in chiral fluorescent sensors[16, 17], polymeric enantioselective catalysts[18], polarized or anisotropic light emissions[19], and helical macromolecules[20]. Besides the axial chirality, the highly soluble and twisted molecular structure of 1,1'-binaphthyl also benefits the conjugated polymers with good solution processability and high luminescent efficiency due to the alleviated self-quenching between the luminophors in amorphous phase[21, 22]. In addition, the changeable dihedral angle from 60° to 120° between the two bulky naphthyl groups of the non-planar binaphthyl offers a feasible control of the effective conjugation length and thus the emission color of the conjugated polymer chain without need to insert an additional bandgap adjusting unit[23]. As a result, binaphthyl-based conjugated polymers were found impressive applications in optoelectronics such as organic light emitting diodes (OLEDs)[24], transistors[25], non-linear optics[26, 27], and solar cells[28]. In these heated research fields of conjugated polymers, however, the effects of chirality on the optoelectronic properties were less addressed and *R*-binaphthyls were used in most reports; it is widely believed that the stereo conformations of the *R*- and *S*- enantiomers have identical or symmetric optical and electronic properties in symmetric environments. In our previous work[29], *(R)*-6,6'-dibromo-2.2'-bis(octyloxy)-1,1'-binaphthyl, however, was found to have higher photoluminescence (PL) quantum efficiency than its *S*-enantiomer in condensed solid state, possibly due to its more twisted molecular structure at both ground and excited states to suppress the intermolecular interaction and the formation of excimers and quenches. This finding gives a new clue for exploring the inherent chiral effects on photophysical properties of optoelectronic materials.

In this paper, we incorporated the two chiral 1,1'-binaphthol enantiomers into the backbone of polyfluorene to further investigate the influence of the different types of main-chain chirality on the photophysical properties of conjugated polymers. The rich optical and electronic properties of polyfluoenes[30, 31], such as high PL efficiency, high charge-carrier mobility, good processability, as well as the ease in excimer and/or fluorenone defect formation, glassy

phase (α-phase) and ordered phase (β-phase) transition[31], and bandgap and colour tuning, provide a satisfied platform for the in-depth structure-property relation investigations. Experimentally by UV-Vis absorption and PL spectra, circular dichroism (CD) spectroscopy, cyclic voltammetry, and quantum efficiency measurements, and theoretically by *ab initio* density functional theory (DFT) calculations and molecular dynamic (MD) simulations, the chirality-photophysical property relationships were systematically investigated. We found obvious differences between the *R*- and *S*- conjugated polymers in that *R*-polymers have higher PL quantum efficiency with higher spectral thermostability while *S*-polymers exhibit stronger ability to suppress the β-phase formation for the construction of color stable amorphous α-phase in the solid state, probably owing to the stronger interchain interaction of *S*-polymers resulted from their more planar chain conformation. The easy introduction and transition of chirality into the backbone of polyfluorene to control the conjugation length, intrachain order, PL efficiency, and dichroism, may update the current understandings on the effects of enantiomers on photophysical properties of main-chain chiral conjugated polymers.

Experimental

Materials. All reagents, unless otherwise specified, were purchased from Aldrich, Across, or Alfa, and used without further treatments. All manipulations involving air-sensitive reagents were performed in an atmosphere of dry N_2. Tetrahydrofuran (THF) and toluene were dried and purified by routine procedures. 9,9-Dioctylfluorene-2,7-dibromide , 9,9-dioctylfluorene-2,7-bis(trimethylene boronate), (*R/S*)-6,6'-Dibromo-2,2'-dihydroxy-1,1'-binaphthyl, (*R/S*)-6,6'-Dibromo-2,2'-bis(octyloxy)-1,1'-binaphthyl and *R/S*-binaphthol-fluorene copolymers were synthesized according to the literatures.[15-16] Both starting chiral compounds (*R*-binaphthol and *S*-binaphthol) for synthesis of chiral (*R/S*)-6,6'-Dibromo-2,2'-dihydroxy-1,1'-dinaphthyl have high stereoregularity (ee>99%). After careful purifications, high purity of the prepared *R*- and *S*-monomers was also identified to be higher than 99.5% by high performance liquid chromatography (HPLC). Detailed synthesis and characterization of the *R*-type binaphthol monomer and its chiral copolymers can be found in our previous report.[14] The *S*-type monomer and copolymers were prepared in the same procedure of the *R*-type.

Copolymerization. To a mixture of 2,2'-(9,9-dioctyl-9H-fluorene-2,7-diyl)bis(1,3,2-dioxaborinane) (1 equiv), dibromo-compounds including (*R/S*)-6,6'-dibromo-2,2'- bis(octyloxy)-1,1'-binaphthyl and 9,9-dioctyl-2,7- dibromofluorene (1 equiv), Aliquat 336, and 2.0 mol% $Pd(PPh_3)_4$, was added a degassed mixture of toluene ([monomer] = 0.25 M) and aqueous 2 M potassium carbonate (3:2 in volume). The mixture was vigorously stirred at 85~90°C for 72 h. After the mixture was cooled to room temperature, the solution was add dropwise to a mixture of methanol and deionized water (220 mL, 10:1 v/v). A fibrous solid was observed and collected by filtration. The solid was dissolved in THF for the purification using flash column chromatography (neutral Al_2O_3 gel, THF) to remove the residual catalyst. The concentrated solution obtained was dropped slowly into methanol (250 mL) again. The fibrous solid was collected and further purified by continuous washing with hot acetone in a Soxhlet apparatus for 2 days to remove oligomers and catalyst residues. Yields: 55–70%. ^{1}H NMR measurements (Figure S5) were performed to identify the actual composition in the copolymer according to the characteristic signals of fluorene (2.11 ppm) and binaphthol (4.00 ppm).

Measurements. Nuclear magnetic resonance (NMR) spectra were collected on a Bruker Ultra Shield Plus 400 MHz instruments with chloroform-D as the solvent and tetramethylsilane (TMS) as the internal standard. Mass spectra of monomers were obtained a Shimadzu GCMS-QP2010. The number-average molecular weight (M_n) and weight-average molecular weight (M_w) of the polymers were measured by gel permeation chromatography (GPC) with Shim-pack GPC-80X columns, using polystyrene as standard and THF as eluent. The UV-vis absorption spectra were recorded on a UV-3600 Shimadzu UV-vis spectrophotometer. The concentrations of the polymer solution (in THF) were adjusted to be lower than 0.01 mg/mL. The thin solid films were prepared by spin-coating on quartz substrates from THF solutions at a spin rate of 3500 rpm. Photoluminescence spectra at various temperatures were measured with Spex Fluorolog-3 Shimadzu spectrophotometers. Circular dichroism (CD) spectroscopies of the chiral polymers in THF solution were carried on JASCO J-810 spectropolarimeter at 25°C, while their CD spectroscopies in thin solid film were measured by a Jasco J-40A spectropolarimeter with a 450 W Xe-lamp as light source**.** The optical rotation of copolymers in THF solution was measured in a WZZ-2S (2SS) digital automatic polarimeter, where the wavelength of sodium lamp was 589.44 nm. Thermogravimetric analyses (TGA) were conducted on a DTG-60 Shimadzu thermal analyst system under a heating rate of 10°C/min and a nitrogen flow rate of 50 cm^3/ min. Differential scanning calorimetry (DSC) was run on a Pyris 1 DSC (PERKIN ELMER Co.) shimadzu thermal analyst system. The glass transition temperature (T_g) were measured on the second curve after heating to 230°C and after cooling to room temperature and the decomposition temperature (T_d) were measured from room temperature to 600°C under nitrogen atmosphere at a heating rate of 10°C/min. The highest occupied molecular orbital (HOMO), the lowest unoccupied molecular orbital (LUMO) and the energy gap between them (E_g) were measured by cyclic voltammetry (CV). The CV measurements were performed at room temperature under argon protection on a CHI660E system in a typical three-electrode cell with a working electrode (glass carbon), a reference electrode (Ag/Ag^+, referenced against ferrocene/ferrocenium (FOC)), and a counter electrode (Pt wire) in an acetonitrile solution of Bu_4NPF_6 (0.10

Table 1. Structure and thermal properties of the chiral conjugated polymers.

Polymer	Feed (%)	Compos. (%)	M_n	M_w/M_n	T_g (°C)	T_d (°C)
R5/S5	5	7.5/4.9	21500/21100	1.8/1.6	51/51	420/423
R10/S10	10	11/9.4	19200/19900	1.7/1.7	53/54	418/420
R20/S20	20	20/19.9	18700/15900	1.6/1.6	57/56	417/418
R30/S30	30	30/29.3	16600/13400	1.5/1.7	62/59	413/415
R50/S50	50	50/50	9280/8500	1.3/1.2	68/67	411/408

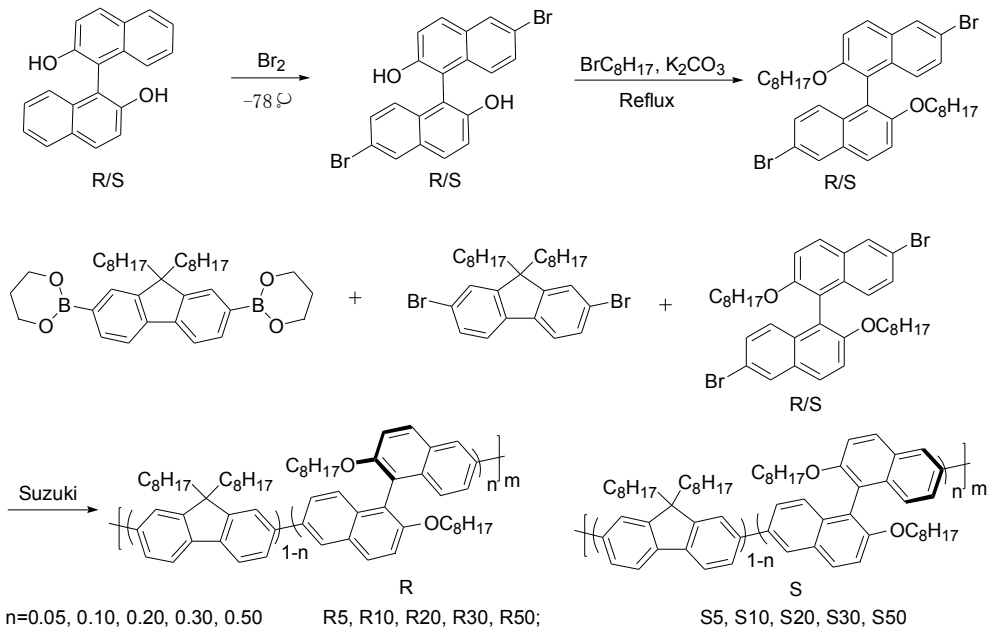

Scheme 1. Synthesis of *R/S*-type chiral conjugated polymers with corresponding *R/S*-binaphthol feed contents of 5, 10, 20, 30, and 50 mol%

M) at a sweeping rate of 100 mV/s. The solutions were bubbled with a constant nitrogen flow for 15 min before measurements. The HOMO/LUMO energy levels of the material are estimated based on the reference energy level of ferrocene (4.8 eV below the vacuum): HOMO/LUMO = $-[E_{onset} - (0.015)] - 4.8$ eV, where the value of 0.015 V is for FOC *vs* Ag/Ag^+ and E_{onset} is the onset potential.

Calculations. Theoretical *ab initio* calculations of the model *R*- and *S*- molecules were performed with Gaussion 09 program using 6-31G(d) basis set. At the single molecular states, the ground-state geometries were fully optimized by the Becke's three-parameter exchange functional along with the Lee Yang Parr's correlation function (B3LYP), followed by harmonic vibration frequency analysis to check that real local minima have been found without imaginary vibrational frequency. The simulated circular dichroism (CD) spectra in vacuum were obtained by time-dependent density functional theory (TDDFT) method of B3LYP based on the optimized ground state geometries adjusted by changing the rotation angles of the two biphenyl rings from 40° to 140°. The corresponding HOMO and LUMO energy levels, energy variation, and oscillator strength were collected according to literature reports[32]. Molecular dynamic (MD) simulations were performed using NAMD (version 2.6) with periodic boundary conditions in NPT ensemble at atmospheric pressure and 300 K. The general amber force field (GAFF) was chosen, because it was developed to cover a wide range of organic species and has good performance in the structure prediction of polymers. A cutoff of 11 Å for non-bonded interactions and a 1 ps equilibration with a time-step of 5 ns were adopted to obtain the energy-minimized polymer conformation. The molecular graphics software VMD was used to visualize the trajectories.

Results and discussion

Synthesis and physical properties. To eliminate the impurity effects, the chiral monomers were prepared from high-standard commercial *R*- and *S*- binaphthols (ee>99%) and carefully purified to remove chemical and chiroptical impurities (purity>99.5%). The chiral conjugated copolymers were then synthesized via Suzuki coupling polycondensation between fluorene and chiral (*R* or *S*) binaphthols comonomers under various molar feed ratios of 5, 10, 20, 30, and 50% (**Scheme 1**), resulting in corresponding copolymers (*R*-polymers or *S*-polymers) of R5, R10, R20, R30, R50 and S5, S10, S20, S30, S50. The polymers were also carefully purified. From the characteristic ^{1}H NMR signals of the repeating units of fluorene (2.11 ppm) and binaphthol (4.00 ppm), the actual compositions of the copolymers were calculated and listed in **Table 1**. The slightly higher *R*-binaphthol content in copolymer than in feed (especially obvious at low feed ratio) suggests the higher copolymerization reactivity of dibromo-(*R*)-binaphthol than dibromofluorene[33]. In contrast, the dibromo-(*S*)-binaphthol shows a little lower copolymerization activity than dibromofluorene under the same Suzuki copolymerization conditions. This difference between the reactivity of the two enantiomers observed experimentally may be the main reason for the higher number-average molecular weights (M_n) of *R*-polymers based on the more reactive *R*-binaphthol. Despite the slight differences in both chain composition and molecular weight, the enantiomorphic *R*- and *S*- copolymers have similar thermal properties (**Table 1**) with slightly increased glass transition temperature (T_g) and decreased decomposition temperature (T_d) after the incorporation of an increased content of bulky and twisty binaphthol units. In comparison with polyfluorene (T_g=51°C, T_d=469°C)[33], the increased T_g of the binaphthol containing conjugated functional polymers along with high T_d (> 400°C) offers stable amorphous states for their optoelectronic applications, since microcrystallization generally shows detrimental effects on luminescence efficiencies[34]. However, the slightly lower liquid crystalline temperature (T_{LC}= 130°C) of R5 than that of polyfluorene (T_{LC}= 175°C)[35] can be easily found but there is no T_{LC} in S5, suggesting that *S*-binaphthol has stronger impact on the packing behaviors of the poly(9,9'-octylfluorene) chains. Excellent solubility of the chiral *R/S*-polymers in common solutions such as chloroform, tetrahydrofuran (THF), toluene, and chlorobenzene was also observed, attributing to both the twisty chiral binaphthol in backbone and to the long alkyl chains of octyl substituents on binaphthol and fluorene. Good thin solid films of the chiral copolymers can be easily constructed by spin-coating on quartz substrates through their

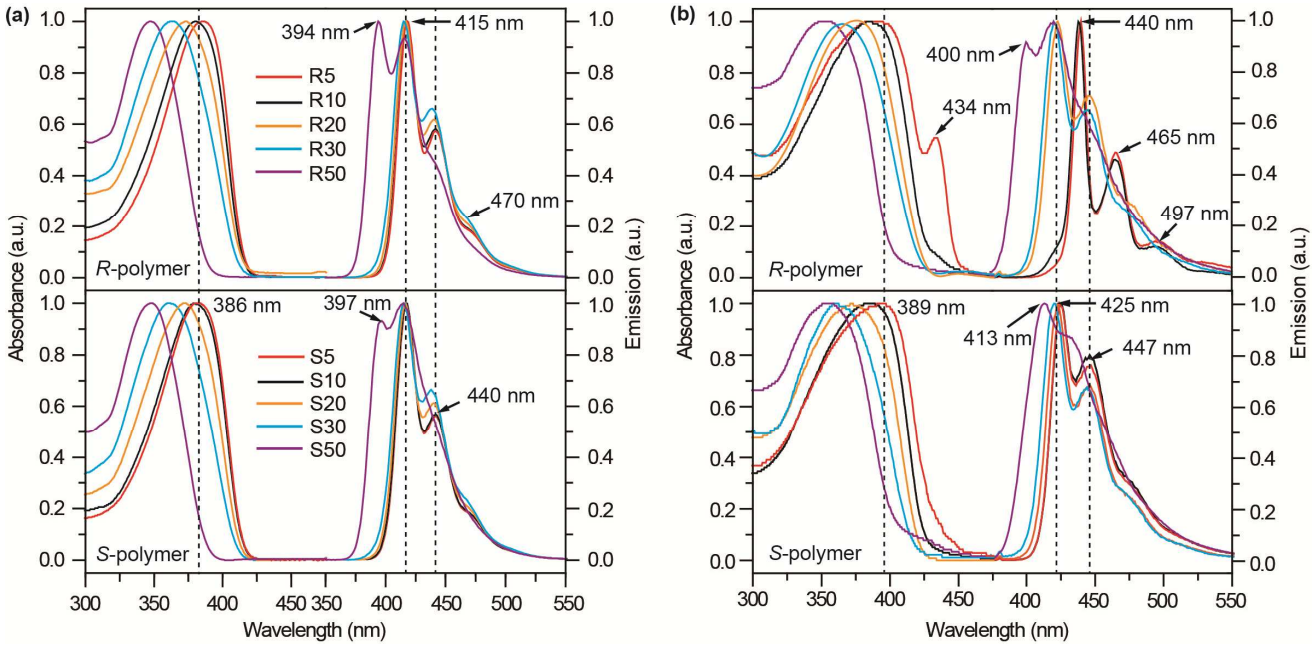

Figure 1. Normalized absorption and photoluminescent spectra of chiral conjugated polymers in dilute THF (**a**) and in thin solid film (**b**).

organic solutions, which is feasible for potential optoelectronic device fabrications[36].

From the literature reports[37] there are certain relations between the synthesis method and the solid film polymer phase. The aggregated structure is intrinsically determined by its chain structure. But there are much more factors[37c, 37d] that have profound effects on the formation of the polymer aggregation phases, such as concentration, solvent, temperature etc. Meanwhile, we have noticed that the Suzuki condensation method had advantage on preparations of binaphthol-based chiral copolymers[14], since it could avoid the racemization during the polymerization. We can further investigate the effects of chiral polymer structure on solid film phase formation under the same aggregation conditions.

Photophysical Properties. The influence of main-chain chirality on the photophysical properties of optoelectronically active conjugated polymers were investigated by ultraviolet-visible (UV-Vis) absorption and photoluminescence (PL) spectra, luminescent quantum efficiency, and PL thermostability in both organic solvent and thin solid film (see Figure 1 and Table 2). The *R*- and *S*- chiral copolymers in dilute THF solution show very similar absorption spectra with an intense band around 384-347 nm associated with π-π* transition of the π-conjugated backbone[14]. The gradual blue shift of the absorption peak from 384 to 347 nm with the increasing content of chiral binaphthol unit in the copolymers from 4.9% to 50%, suggests that (1) the twisty binaphthol unit partly breaks and decreases the effective conjugation length of polyfluorene backbone and (2) the *R*- and *S*- binaphthol enantiomers have identical effects on the conjugation length tuning of polyfluorene. The significant conjugation length reduction happens when binaphthol content is higher than 30 mol%, accompanied by not only the significantly blue-shifted absorption peak but also the significantly enlarged optical bandgap (E_g^{Opt}) judged from the onset of absorption spectra. This was further confirmed by their PL spectra in THF (Figure 1a). R50 and S50 show a new luminescence peak around 395 nm, while the other chiral copolymers exhibit similar 0-0, 0-1, and 0-2 vibronic emissive transitions of polyfluorene with corresponding emission peaks around 415, 440, and 470 nm[30]. The single molecular photophysical properties of the binaphthol copolymers measured in THF solution indicates that the conjugation length of polyfluorene can tolerate a large incorporation ratio of binaphthol up to 30 mol% without obvious obstacles on both emission peaks and luminescent quantum yields (**Table 1**), suggesting that binaphthol is a good building block for the construction of optoelectronic conjugated polymers.

In the solid thin film state (**Figure 1b**), however, *R*- and *S*-polymers behave quite differently in both absorption and emission properties. Despite the gradual blue-shift of absorption peaks due to the increased binaphthol incorporation ratio, a new peak (or shoulder) associated with the β-phase absorption appears at 434 nm in R5 film. The characteristic emission bands of β-phase was also observed in the PL spectra of R5 and R10, located at 440, 465, and 497 nm, which are very close to that of pure poly(9,9'-dioctylfluorene) film[33]. In sharp contrast, the S-polymers do not show visible β-phase signals even when the incorporation ratio of chiral binaphthol is low, suggesting that the *S*-enantiomer is a strong suppressor towards the formation of intrachain ordered β-phase in polyfluorenes even when its content is lower than 5%. When the content of *R*-enantiomer of binaphthol is higher than 10%, the β-phase is completely eliminated and the copolymers show identical emission of α-phase polyfluorene film around 425 and 447 nm, indicating that lumniophor of the copolymers has identical emission properties. This phenomenon is more apparent in S5, S10, S20, and S30; they have very similar PL spectra regardless of the changing composition and shifted absorption spectra of the copolymers. Only in the alternative copolymers of R50 and S50 at the high loading content of binaphthol units, the emission peaks are only slightly blue-shifted due to the restricted main-chain conjugation of fluorene copolymers, indicating again the large tolerance of the PL properties after the binaphthol incorporation. The identical PL spectra with identical Commission International de L'Eclairage (CIE) in solution and of *S*-polymer films (**Table 2**) when the composition of binaphthol is changing in a wide range (30 mol%) provide a good platform for independent tuning[38a] of the

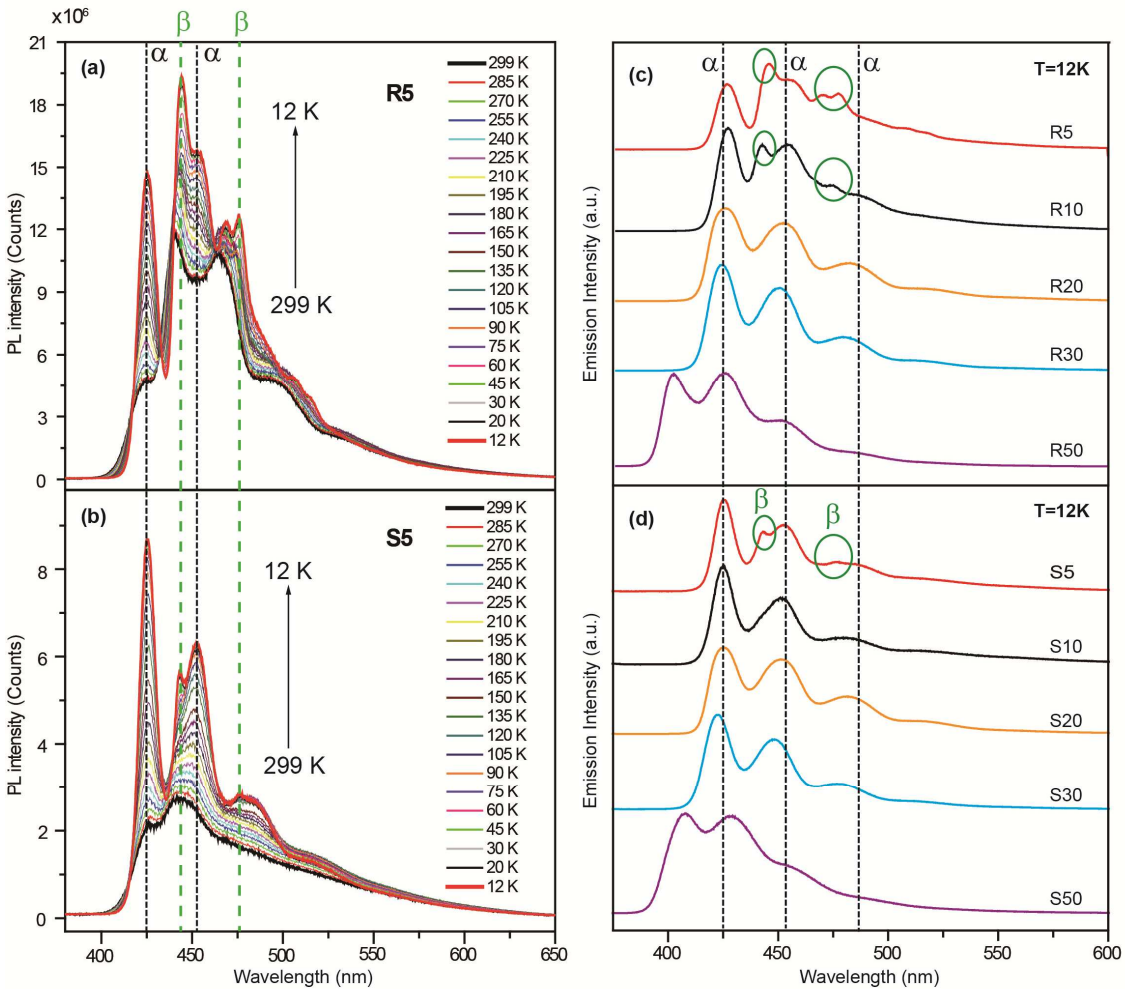

Figure 2. PL spectra of R5 (**a**) and S5 (**b**) films when temperature changes from 299 K to 12 K and PL spectra of all the *R*- (**c**) and *S*- (**d**) conjugated polymers at 12 K when excited at 350 nm.

interested properties of the chiral units without influence on the photophysical properties of the chiral conjugated copolymers.

In order to get a deep understanding of the different effects of *R*- and *S*- enantiomers on the intrachain ordered β-phase emission in the condensed solid film, their temperature-dependent photoluminescence behaviors (**Figure 2**) were investigated. As we reported previously[38b], when the temperature drops from 290 to 12 K (**Figure S6**), poly(9,9'-dioxylfluorene) film shows gradually enhanced emissions with fixed 0-0 vibronic transition bands of α-phase (424 nm) and β-phase (442 nm) state, while the 0-1 and 0-2 transition resulted emission peaks either β-phase-related or α-phase-related gradually red-shift from 447 nm (α-phase) and 465 and 497 nm (β-phase) at room temperature to 454 nm (α-phase) and 470 and 505 nm (β-phase) at 12 K, respectively. The emission enhancement due to reduced non-irradiative deactivation processes at low temperatures was also observed in both types of the chiral conjugated polymers. However, the emission intensities of R30, S30, R50, and S50 decrease at very low temperature (<60 K), suggesting that a new non-irradiative species has been formed which overwhelms the benefits achieved for irradiative emission at low temperature. More interestingly, the emission decrease of *S*-polymers is more severe than that of enantiomeric *R*-polymers (**Figure S7**), indicating that the formation of the non-irradiative species is chirality dependent. The α-phase and β-phase emissions of the chiral conjugated polymers also show different temperature-dependent properties in comparison with that of poly(9,9'-dioxylfluorene)[38b]. Only the 0-0 transition of α-phase (424 nm) is relatively unchanged upon temperature variation; the emission wavelengths of β-phase are very sensitive to the chiral binaphthol incorporation even when the composition is as low as 5%. Consequently, β-phase emission disappears in the copolymers when the binaphthol content is higher than 10%, in accordance with that found at the room temperature. A weak β-phase emission of S5 that overlooked at room temperature was observed at 12 K. However, the difference between the β-phase emission of *R*- and *S*- polymers are still significant at low temperature (**Figure 2c**), which further confirms that the *S*-binaphthol is a stronger suppressor than *R*-binaphthol towards the formation of β-phase in polyfluorenes.

To investigate the influence of chirality on the photophysical stability, PL spectra of the spin-coated chiral polymer films annealed at different temperatures were tested. There is no change in PL spectra of all the chiral copolymers when they were annealed below 200°C in nitrogen, indicating increased photophysical stability after binaphthol incorporation than that in polyfluorene[14]. However, after the films were

annealed at 200°C in air for 10 h (**Figure 3**), obvious green band around 520 nm that typically observed in poly(9,9'-octylfluorene), appeared in copolymers with 5% and 10% content of chiral binaphthol. Excellent spectral thermal stability was found in R20 and R30, which shows almost no change in the PL spectra before and after annealing at 200°C in air for 10 h. The significantly stabilized PL spectra after both *R*- and *S*-binaphthol incorportation may be because of the presence of the twisty conformation of binaphthol units, which restrict the close packing of the polymer chains and reduce the probability of interchain interactions by suppressing the formation of aggregates and excimers in polymers. Nevertheless, *R*-polymers generally have higher stability than the corresponding *S*-polymers, demonstrating the different effects of the chirality of enantiomers since their copolymers have similar compositions and molecular weights.

The electrochemical properties of the chiral copolymers were measured by cyclic voltammetry (CV). The chiral conjugated polymers show reversible electrochemical redox CV curves and from the onset potential of electrochemical reduction and oxidation, the LUMO and HOMO can be calculated respectively (**Table 2**) on the basis of the reference energy level of ferrocene[39]. The *R*- and *S*- binaphthol copolymers show very close HOMO and LUMO energy levels and electronic bandgaps (E_g^{EL}) with low variation (<0.15 eV) even when the content of binaphthol is as high as 50% in alternative copolymers of R50 and S50. This interesting feature provides binaphthol-containing optoelectronic materials with intriguing feasibility in selective performance optimization of the materials without disturbance on their electronic band structures.

The luminescent quantum efficiencies (Φ_F) of the chiral conjugated polymers in both solution and thin solid film were measured by 9,10-diphenylanthracene (Φ_{360} = 0.9) as reference standard in dilute cyclohexane solutions (Table 1) and by integral sphere respectively to investigate the influence of the chirality. High and similar Φ_Fs in solution for boh *R*- and *S*-polymers were obtained, while in condensed film state, *R*-polymers generally show higher Φ_F than the corresponding *S*-polymers. In our previous study[29], *S*-binaphthyl was experimentally identified to have lower PL efficiency due to its stronger tendency to form dimers and excimers with its more planar molecular structure especially at excited states than *R*-binaphthyl. In this study, it seems that the *R*- and *S*- polymers can inherit this feature of their monomers; this again breaks the generally accepted concept that enantiomers should have the same physical properties in a symmetrical environment. It seems that the influence of different chirality from the enantiomers can not be ignored when they are selected as building blocks for the construction of optoelectronic materials.

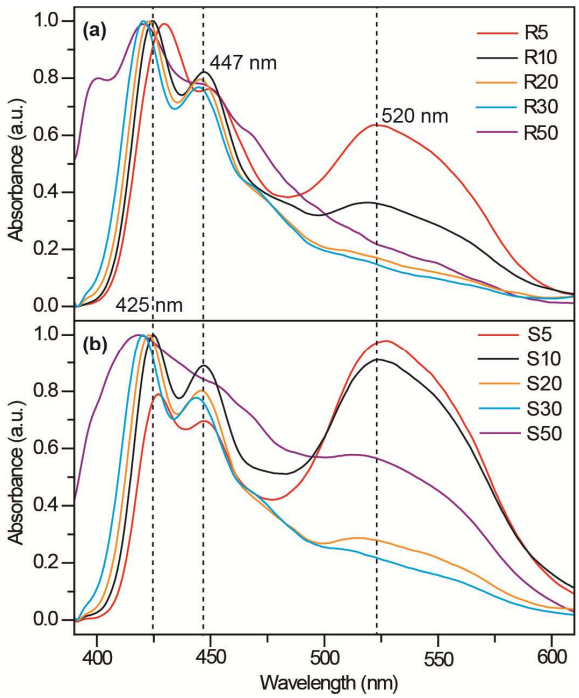

Figure 3: Normalized PL spectra of *R*-polymers (**a**) and *S*-polymers (**b**) annealed at 200℃ in air for 10 h in thin film.

Circular Dichroism Properties. To clarify the chiroptical properties of the chiral conjugated polymers, specific rotations ($[\alpha^{25}_D]$) and the circular dichroism (CD) spectra in both solution and thin solid film were measured. From **Table 3**, the absolute values of $[\alpha^{25}_D]$ in THF increase with increasing content of binaphthol in both *R*- and *S*-polymers, due to a propagating helical chain conformation of the copolymers.[40] But the negative $[\alpha^{25}_D]$s of *R*-copolymers are

Table 2. Optical and electrochemical properties of the chiral conjugated polymers at room temperature.

Polym.	$UV_{\lambda max}$ (nm)		E_g^{Opt}	$PL_{\lambda max}$ (nm)		Φ_F (%)		CIE (x,y)		HOMO/LUMO	E_g^{EL}
	THF	Film	(eV)	THF	Film	Sol.[a]	Film	THF	Film	(eV/eV)	(eV)
R5	386	389,434	2.95	418,441	440,465,497	93	24.3	(0.157, 0.034)	(0.155, 0.095)	-5.77/-2.17	3.60
S5	384	394	2.88	417,442	425,447	89	17.0	(0.157, 0.034)	(0.154, 0.064)	-5.77/-2.19	3.58
R10	380	383(434)	2.96	418,442	438,464,493	109	23.6	(0.157, 0.034)	(0.150, 0.058)	-5.76/-2.16	3.60
S10	379	385	2.92	417,442	424,446	110	11.8	(0.157, 0.035)	(0.154, 0.064)	-5.76/-2.16	3.60
R20	373	374	2.98	417,440	423,446	110	22.5	(0.157, 0.035)	(0.153,0.063)	-5.75/-2.16	3.59
S20	372	372	2.94	416,440	423,446	99	22.9	(0.157, 0.035)	(0.155, 0.053)	-5.77/-2.15	3.62
R30	363	364	3.00	415,439	420,445	109	20.8	(0.157, 0.036)	(0.154, 0.055)	-5.74/-2.14	3.60
S30	361	362	2.97	415,438	420,444	70	16.2	(0.157, 0.036)	(0.156, 0.051)	-5.74/-2.10	3.64
R50	347	352	3.17	394,416	400,420	87	23.6	(0.159, 0.030)	(0.155, 0.062)	-5.72/-2.10	3.62
S50	347	353	3.10	397,415	413(431)	86	15.0	(0.158, 0.032)	(0.155,0.063)	-5.71/-2.01	3.70

[a] Φ_F in cyclohexane was estimated using 9,10-diphenylanthracene (Φ_F = 0.9) as standard.

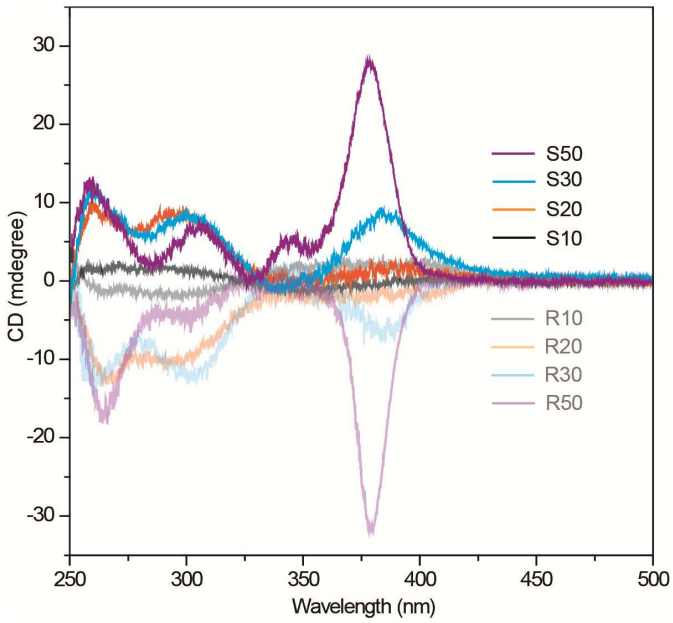

Figure 4: CD spectra of the chiral conjugated polymers in thin solid films at room temperature.

opposite to their monomer with positive [α^{25}_D]; this opposition was also found in *S*-copolymers. The absolute values of [α^{25}_D] of *S*-polymers are relatively larger than that of corresponding *R*-polymers. The relationship between [α^{25}_D] (Y) and content of binaphthol (X) in copolymers can be described in the following line-equations: Y = -16.84-4.084X and Y = 32.02+4.433X for *R*- and *S*-polymers respectively. Both intercept and slope of the equation of *S*-polymers are larger than that of *R*-polymers, indicating relatively more sensitive change of [α^{25}_D] towards the content of *S*-binaphthol.

R-binaphthol comonomer show positive CD signals from 280 to 340 nm, while *S*-binaphthol has the negative ones in a mirror image as typically observed in enantiomers[14]. In stark contrast, CD spectra in polymers (**Figure 4**) show only negative and new-emerged CD signals around 255, 290, and 375 nm in *R*-polymers, while in *S*-polymers only positive ones in mirror images of that of *R*-polymers were observed in both THF solution and film, providing direct evidence for the successful introduction and transfer of the chirality into the conjugated polymers. This transition between monomer and polymer confirmed by both CD spectra and [α^{25}_D] indicates the formation a secondary structure[41] probably due to the transfer of the chirality in the polymer backbone. Due to the high enantiomerization barrier of binaphthols[42], they are stable enough to survive the polymerization conditions and main-chain relaxation to keep their intrinsic chirality and induce new ones after interactions with the other units in the conjugated backbone[10]. With the increase of the chiral binaphthol content, the CD peak at short wavelength (around 290 nm) is red-shifted and slightly decreased, whereas the peak at the longer wavelength (around 375 nm) is blue-shifted but significantly enhanced. However, the enhancement requires a high content of chiral binaphol units in copolymers (more than 20%) to establish the new-emerged CD signals of the chiral conjugated polymers in thin films.

Theoretical investigations and discussions. For in-depth understanding of the chiroptical properties of the binaphthol-containing chiral conjugated polymers, the TDDFT method was used to predict CD spectra based on the pre-optimized geometries of the model compounds (*R*- and *S*- trimers in **Figure 5a**) of R30 and S30 at B3LYP/6-31G(d) level, since R30 and S30 have the typical molecular structures of the copolymers and relatively higher CD intensities with stable PL properties. The DFT optimized *R*- and *S*- trimer structures at the ground state are not perfect enantiomers as expected; the dihedral angle between the two naphthalene moieties in *R*-oligomer is 91.9°, while that in *S*-oligomer is -92.5°. This slightly larger dihedral angle was also observed in *S*-binaphthols in our previous studies[29], which suggests that the molecular conformation of *S*-binaphthols is more planar and apt to form dimers at the ground states and excimers at excited states upon photoexcitation. The calculated dihedral angles are both close to 90°, which may prevent the effective π-electron interaction and lead to the breakage of the main-chain conjugation as discussed above. However, in polymers this angle may be varied due to spatial hindrance of the repeating units and the entanglement of polymer chains. The influence of this dihedral angle change on the molecular energy and CD spectra was investigated theoretically (**Figure 5**). In a low energy barrier of 0.3 eV, the dihedral angle can be varied from 60° to 120°, suggesting the high flexibility of the binaphthol units and thus the polymer chain. However, the calculation results indicate that this feasible change of the dihedral angle could result in significantly different CD spectra; the shorter wavelength CD peak around 290 nm becomes red-shifted and

Table 3. Specific rotation ([α^{25}_D]) in THF and peak wavelength of CD spectra (λ_{max}) of the chiral copolymers in both THF and thin film.

Copolymer	Specific Rotation		λ_{max} (nm)	
	C (g/100 mL)	[α^{25}_D] (deg.)	Solution	Film
R5/S5	0.031/0.035	-35.8/47.9	280,391/387	-
R10/S10	0.032/0.027	-52.0/61.1	282,387/383	-
R20/S20	0.025/0.022	-87.6/146.4	289,379/291,378	257,291/259,293
R30/S30	0.025/0.029	-170.4/171.1	289,373/293,374	253,299,384/257,297,381
R50/S50	0.036/0.021	-208.1/243.4	295,365/299,367	265,305,382/259,304,378

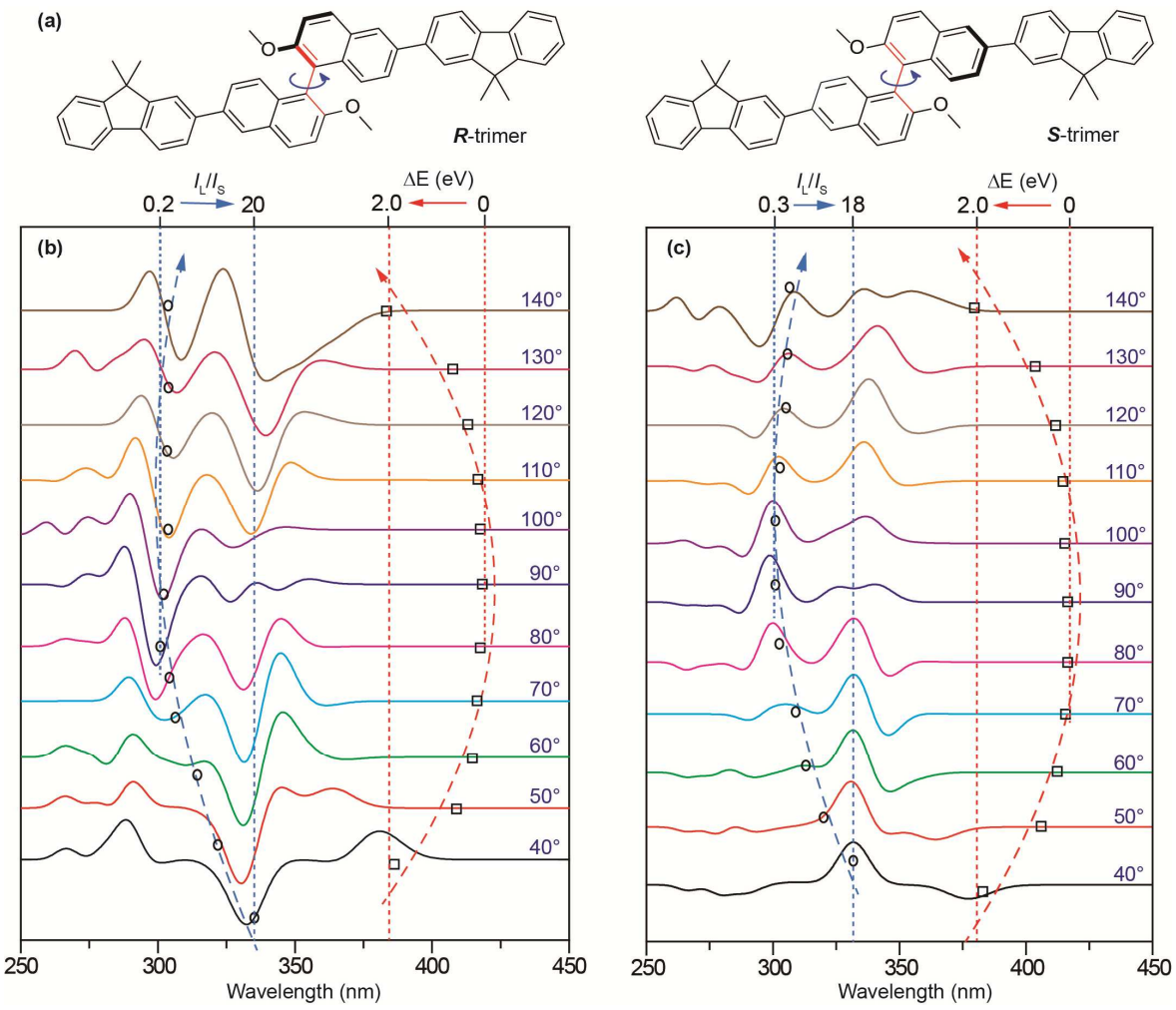

Figure 5: The model compounds (*R*- and *S*- trimers, **a**) of R30 and S30 with their theoretical prediction of the relations (**b** and **c**) between the dihedral angles (from 40° to 140°) and the CD spectra, the intensity ratio (I_L/I_S) of the peak in longer wavelength (I_L) and that in short one (I_S), and molecular energy variation (ΔE).

weakened, while the longer wavelength CD peak around 330 nm is blue-shifted and enhanced, when the dihedral angle increases from 90° to 120° or decreases from 90° to 60°. Comparing this theoretical results on the intensity ratio of the longer and the shorter wavelengths (I_L/I_S) with the experimentally obtained ones (about 0.7 and 1.0 for R30 and S30 respectively, see **Figure 4**), it can be proposed that the real dihedral angles in R30 and S30 are in the range from 80° to 110° and the angle of R30 should has smaller variation around its most stable conformation of 91.9° than that of S30 due to its lower I_L/I_S observed experimentally. Since the low dihedral angle will lead to a crowd and unstable chain conformation, the actual dihedral angle in the copolymers is supposed to be larger than 100° instead of lower than 90°, and *S*-polymers have larger dihedral angle than *R*-polymers.

Considering that the CD spectrum is sensitive to the polymer conformation[43] and the model compounds of *R*- and *S*-trimmers do not have appropriate structures and sufficient chain length to represent R30 and S30 respectively, MD simulations were performed to investigate the polymer chain structures of these chiral conjugated copolymers at 300 K based on *R*- and *S*-21mers with similar backbone compositions and substitutions of the corresponding copolymers (**Figure 6**). The dihedral angle between the two naphthalene moieties controls the main-chain chirality and conjugation length, while the *n*-alkyl substituents on both binaphthol and fluorene guide the packing behaviors such as the formation of α-phase or β-phase in the condensed solid state. The MD predicted equivalent trajectories of the single polymer chains at 300K give a good theoretical support of our above assumptions that dihedral angles are generally larger than 100° (except for R50) and *S*-polymers have larger dihedral angles than *R*-polymers. The larger dihedral angle of *S*-polymer suggested by both DFT calculations and MD simulations, makes the conjugated backbone more planar and the chain structure more open. The more planar backbone conformation results in longer effective conjugation length and lower optical band-gap of the *S*-polymers (**Table 2**); while the more open chain structure leads to stronger interchain interaction in *S*-polymers especially in condensed phase, which will disturb the intrachain ordering

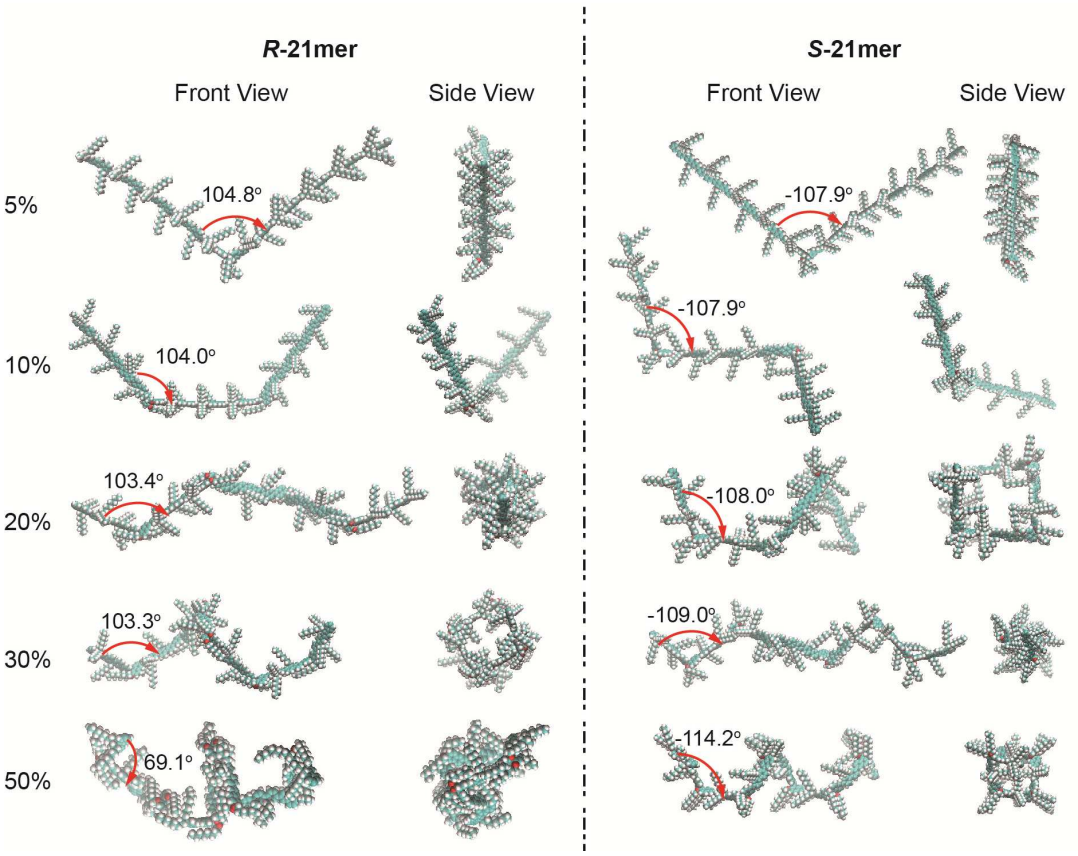

Figure 6: Front view and side view of the MD simulated chiral main-chain conformations based on the *R*- and *S*- 21mer with similar compositions of the experimental copolymers.

process induced by the *n*-alkyl substituents to form β-phase and facilitate the formation of low efficient and unstable excimers, resulting in the lower content of β-phase in *S*-polymers (Figure 2) and the lower luminescent quantum efficiency (**Table 2**) and spectrum thermal stability **(Figure 3**) of the *S*-polymers, respectively.

However, the inherent reason for the different planarity of *R*- and *S*- monomers and polymers revealed by DFT and MD calculations is still need to be investigated experimentally. In addition, the effects of chemical and enantiomeric impurities, although controlled to be lower than 0.5% and 1.0% respectively, may still lead to observed difference in solid state. Nevertheless, these factors might not be strong enough to dissimulate the relations between the chirality and the photophysical properties of the conjugated polymers observed from this systematic study on *R*- and *S*- conjugated polymers with similar chain compositions and molecular weights. In a controlled experiment, we deliberately mixed *R*- and *S*-binaphthols to prepare partially racemic conjugated polymer with high enantiomeric impurities. The prepared R4S1, where *R*-binaphthols is 4% and *S*-one is 1%, shows obviously higher α-phase emission than R5 but still with β-phase emission at the identical conditions of R5 and S5 (**Figure S8a**), suggesting the artificially incorporated 1% *S*-binaphthols partially disturbed the β-phase formation due to its stronger β-phase suppressibility. Considering the possible effects of the different interactions between the chiral polymer and the quartz surface on the photophysical properties, the PL spectra were further collected from the chiral polymer films (R5, S5, and R4S1) spin-coated on the surfaces of silicon wafer and mica sheet (**Figure S8b and S8c**). The same trend of their PL variations was observed, suggesting that the PL difference at solid state is originally from their different molecular chirality. The thermostability of R4S1 is also in between R5 and S5, which is stronger than S5 but lower than R5, as indicated from their PL spectra after annealing at 200℃ in air for 10 h (Figure S9). R4S1 film has higher PL quantum efficiency (18.4%) than S5 (17.0%) and lower than R5 (24.3%), which is in consistence with the findings in enantiomeric pure copolymers that *R*-chiral luminescent polymers generally has higher PL quantum efficiency than the *S*-counterpart.

Conclusions

A series of chiral binaphthol-fluorene conjugated copolymers were successfully synthesized by Pd-catalyzed Suzuki polycondensation to covalently incorporate the different axially chiral *R* and *S*-binaphthol into the polyfluorene backbone. Based on the careful control of the chemical and chiroptical impurities, the influences of the main-chain chiral conjugated copolymers on the chain composition, thermal properties, UV-vis absorption and PL spectra at various temperatures, PL efficiency, electrochemical properties, and circular dichroism spectra in both solution and film can be experimental investigated. It reveals that the *R*- and *S*- chirality were preserved and transferred to the conjugated backbone; the chirality takes its effects in various aspect of the photophysical properties of the chiral conjugated polymers, including that (1) the thermostability was significantly improved in comparison

with polyfluorene even when the content of binaphthol is as low as 5 mol%, and *R*-polymers have relatively better spectral thermostability than *S*-polymers; (2) the incorporated binaphthol units greatly suppress the formation of the β-phase, and *S*- chirality shows stronger suppressing ability than *R*-chirality; (3) the chiral conjugated polymers have very high luminescent efficiencies, and *R*-polymers possess higher PL quantum efficiency than *S*-polymers in condensed state. The theoretical studies based on both DFT calculations and MD simulations show that the main possible reason for the different photophysical properties induced by the main-chain chirality may be that the *S*-binaphthol has more planar molecular structure that favors interchain interaction for the formation of low efficient and unstable excimers or quenches. These findings, although quite different from the current general understandings on enantiomers, may provide new clues for the fundamental studies and applications of chiral conjugated polymers.

Acknowledgements

The present work was supported by the National Natural Science Foundation of China (Project No. 21274065, 21304049, 61136003, and 51173081), Natural Science Foundation of Jiangsu Province (BK2011751), the Ministry of Education of China (No. IRT1148), a project funded by the priority academic program development of Jiangsu higher education institutions (PAPD), the Program for Postgraduates Research Innovations in University of Jiangsu Province (CXLX11_0419, CXZZ11_0412, and CXZZ12_0455), and Scientific Research Foundation of Nanjing University of Posts and Telecommunications (NY210017, NY210046), and by the Grant-in-Aid for the Scientific Research from the Japan Society for Promotion of Science (Project No. 22560013).

Notes and references

[a] Institute of Advanced Materials, Key Laboratory for Organic Electronics & Information Displays (KLOEID), Nanjing University of Posts and Telecommunications (NJUPT), Wenyuan Road 9, Nanjing 210023, China.

[b] Faculty of Engineering, Kyoto Sangyo University, Kamigamo, Kyoto 603-8555, Japan.

[c] Jiangsu-Singapore Joint Research Center for Organic/Bio- Electronics & Information Displays and Institute of Advanced Materials, Nanjing Tech University, Nanjing 211816, China.

Electronic Supplementary Information (ESI) available: The detailed characterization of the chiral monomers and conjugated polymers, and the temperature-dependent PL spectra of poly(9,9'-octylfluorene) and the chiral conjugated copolymers. See DOI: 10.1039/b000000x/

Reference:

1 G. L. Hamilton, E. J. Kang, M. Mba, F. D. Toste, *Science*, **2007**, 317(5837), 496-499.
2 T. W. Hambley, *Coordin. Chem. Rev.*, **1997**, 166, 181-223.
3 J. S. Seo, D. Whang, H. Lee, S. I. Jun, J. Oh, Y. J. Jeon, K. Kim, *Nature*, **2000,** 404(6781), 982-986.
4 Y. Kubo, S. Maeda, S. Tokita, M. Kubo, *Nature*, **1996,** 382(6591), 522-524.
5 K. Ohmatsu, M. Ito, T. Kunieda, T. Ooi, *Nat. Chem.*, **2012**, 4(6), 473-477.
6 D. Cornelis, E. Franz, I. Asselberghs, K. Clays, T. Verbiest, G. Koeckelberghs, *J. Am. Chem. Soc.*, **2011**, 133(5), 1317-1327.
7 A. Shockravi, A. Javadi, E.Abouzari-Lotf, *RSC Adv.*, **2013**, 3(19), 6717-6746.
8 P. Deria, C. D. Von Bargen, J. H. Olivier, A. S. Kumbhar, J. G. Saven, M. J. Therien, *J. Am. Chem. Soc.*, **2013**, 135(43), 16220-16234.
9 L. Pu, *Acta Polym.*, **1997**, 48(4), 116-141.
10 Y. Yang, Y. Zhang, Z. Wei, *Adv. Mater.*, **2013**, 25(42), 6039-6049.
11 L. Pu, *Chem. Rev.*, **1998**, 98(7), 2405-2494.
12 K. Kawabata, H. Goto, *J. Mater. Chem.*, **2012**, 22(44), 23514-23524.
13 Z. T. Liu, Y. Y. Huang, Y. Li, Y. M. He, Q. H. Fan, *J. Polym. Sci. Part a: Polym. Chem.*, **2011,** 49(3), 680-689.
14 Z. An, J. Yin, N. Shi, H. Jiang, R. Chen, H. Shi, W. Huang, *J. Polym. Sci. Part a: Polym. Chem.*, **2010**, 48(17), 3868-3879.
15 L. Ma, Q. S. Hu, D. Vitharana, C. Wu, C. Kwan, L. Pu, *Macromolecules*, **1997**, 30(2), 204-218.
16 Y. Z. Wu, X. R. Mao, X. Ma, X. B. Huang, Y. X. Cheng, C. J. Zhu, *Macromol. Chem. Phys.*, **2012**, 213(21), 2238-2245.
17 Y. Liu, Q. Miao, S. W. Zhang, X. B. Huang, L. F. Zheng, Y. X. Cheng, *Macromol. Chem. Phys.*, **2008,** 209(7), 685-694.
18 Y. Chen, S. Yekta, A. K. Yudin, *Chem. Rev.*, **2003,** 103(8), 3155-3211.
19 K. Watanabe, H. Iida, K. Akagi, *Adv. Mater.*, **2012,** 24(48), 6451-6456.
20 E. Yashima, K. Maeda, H. Iida, Y. Furusho, K. Nagai, *Chem. Rev.*, **2009,** 109(11), 6102-6211.
21 Q. G. He, H. Z. Lin, Y. F. Weng, B. Zhang, Z. M. Wang, G. T. Lei, L. D. Wang, Y. Qiu, F. L. Bai, *Adv. Funct. Mater.*, **2006,** 16(10), 1343-1348.
22 Y. Zhou, Q. G. He, Y. Yang, H. Z. Zhong, C. He, G. Y. Sang, W. Liu, C. H. Yang, F. L. Bai, Y. F. Li, *Adv. Funct. Mater.*, **2008,** 18(20), 3299-3306.
23 D. C. Jeong, H. Lee, K. S. Yang, C. Song, *Macromolecules*, **2012,** 45(24), 9571-9578.
24 Y. Q. Liu, G. Yu, A. Jen, Q. S. Hu, L. Pu, *Macromol. Chem. Phys.*, **2002,** 203(1), 37-40.
25 Y. Yang, R. C. Da Costa, M. J. Fuchter, A. J. Campbell, *Nat. Photon.*, **2013,** 7(8), 634-638.
26 K. Konishi, M. Nomura, N. Kumagai, S. Iwamoto, Y. Arakawa, M. Kuwata-Gonokami, *Phys. Rev. Lett.*, **2011,** 106(0574025).
27 Y. Zeng, C. S. Wang, X. B. Huang, Y. X. Cheng, *J. Appl. Polym. Sci.*, **2012,** 124(4), 2867-2870.
28 B. Pokhrel, S. Konwer, A. Dutta, M. K. Huda, B. Ghosh, S. K. Dolui, *J. Appl. Polym. Sci.*, **2011,** 122(5), 3316-3321.
29 T. Tsuboi, Z. An, Y. Nakai, J. Yin, R. Chen, H. Shi, W.Huang, *Chem. Phys.*, **2013,** 412, 34-40.
30 U. Scherf, E. List, *Adv. Mater.*, **2002,** 14(7), 477-487.
31 R. Chen, C. Zheng, Q. Fan, W. Huang, *J. Comput. Chem.*, **2007,** 28(13), 2091-2101.
32 (a) M. Yan, Y. Tao, R. Chen, C. Zheng, Z. An, W. Huang, *RSC Adv.*, **2012,** 2(20), 7860-7867. (b) J. Yin, R. Chen, S. Zhang, H. Li, G. Zhang, X. Feng, Q. Ling, W. Huang, *J. Phys. Chem. C*, **2011,** 115(30), 14778-14785.
33 (a) L. R. Tsai, C. W. Li, Y. Chen, *J. Polym. Sci. Part a: Polym. Chem.*, **2008,** 46(17), 5945-5958. (b) R. Chen, Q. Fan, S. Liu, R. Zhu, K. Pu, W. Huang, *Synth. Met.*, **2006,** 156(18–20), 1161-1167
34 L. X. Zheng, R. C. Urian, Y. Q. Liu, A. Jen, L. Pu, *Chem. Mater.*, **2000,** 12(1), 13-15.
35 D. Neher, *Macromol. Rapid Comm.*, **2001,** 22(17), 1366-1385.
36 H. Zheng, Y. N. Zheng, N. L. Ai, N. Liu, Q. Wang, S. Wu, J. H. Zhou, D. G. Hu, S. F. Yu, S. H. Han, W. Xu, C. Luo, Y. H. Meng, Z. X. Jiang, Y. W. Chen, D. Y. Li, F. Huang, J. Wang, J. B. Peng, Y. Cao, *Nat. Comm.*, **2013,** 4(1971), 10.1038/ncomms2971.
37 (a) G. Wei, S. Zhang, C. Dai, Y. Quan, Y. Cheng, C. Zhu, *Chem. Eur. J.*, **2013**, 19(47), 16066-16071. (b) F. Song, N. Fei, F. Li, S. Zhang, Y. Cheng, C. Zhu, *Chem. Commun.* **2013**, 49, 2891-2893. (c) A. Satrijo, S. C. J. Meskers, T. M. Swager, *J. Am. Chem. Soc.*, **2006**, 128, 9030-9031. (d) M. Grell, D. D. C. Bradley, G. Ungar, J. Hill, and K. S. Whitehead, *Macromolecules,* **1999**, 32, 5810-5817.
38 (a) Y. Tao, J. Xiao, C. Zheng, Z. Zhang, M. Yan, R. Chen, X. Zhou, H. Li, Z. An, Z. Wang, H. Xu, W. Huang, *Angew. Chem. Int. Edit.*, **2013,** 52(40), 10491-10495. (b)H. F. Shi, Y. Nakai, S. J. Liu, Q. Zhao, Z. F. An, T. Tsuboi, W. Huang, *J. Phys. Chem. C*, **2011,** 115(23), 11749-11757.
39 R. Chen, R. Zhu, Q. Fan, W. Huang, *Org. Lett.*, **2008,** 10(13), 2913-2916.
40 S. W. Sisco, J. S. Moore, *Chem. Sci.*, **2014,** 5(1), 81-85.
41 B. Fu, X. Zhang, Z. Wang, Y. Bai, H. Liu, Y. Zhou, A. Song, F. Song, Z. Zhang, *Polym. Int.*, **2014**, 63(4): 796-800.
42 J. Sanz García, C. Lepetit, Y. Canac, R. Chauvin, M. Boggio-Pasqua, *Chem Asian J*, **2013,** 9(2), 462–465.
43 C. Niezborala, F. Hache, *J. Am. Chem. Soc.*, **2008,** 130(38), 12783-12786.

Graphical Abstract

Main-chain Chirality and Photophysical Property Relations in Chiral Conjugated Polymers

Chao Zheng,[a] Zhongfu An,[a] Yosuke Nakai,[b] Taiju Tsuboi,*[b, c] Yang Wang,[a] Huifang Shi,[a,c] Runfeng Chen,*[a] Huanhuan Li,[a] Yimu Ji,[a] Junfeng Li,[a] Wei Huang*[a, c]

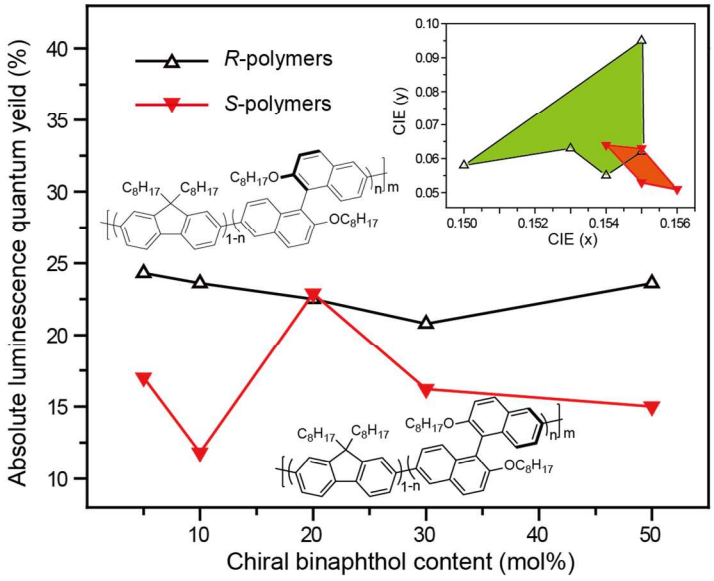

The different effects of binaphthyl enantiomers on photophysical properties of chiral conjugated polymers were observed and analyzed for chiroptic investigations.